ELSEVIER

Synthetic Metals 113 2000 281–287

SYNTHETIC METALS

www.elsevier.com/locate/synmet

Travelling-wave lasing of TPD solutions and neat films

W. Holzer [a], A. Penzkofer [a,*], H.-H. Hörhold [b,c]

[a] *Institut II-Experimentelle und Angewandte Physik, Universität Regensburg, Universitätsstraße 31, D-93053 Regensburg, Germany*
[b] *Innovent Technologieentwicklung e.V., D-07745 Jena, Germany*
[c] *Institut für Organische Chemie und Makromolekulare Chemie der Universität Jena, Humboldtstrasse 10, D-07743 Jena, Germany*

Received 28 January 2000; received in revised form 13 March 2000; accepted 16 March 2000

Abstract

The travelling-wave lasing action amplified spontaneous emission ASE of the electrically active triphenylamine dimer *N,N*′-diphenyl-bis 3-methylphenyl -biphenyl-4,4′-diamine TPD in 1,4-dioxane solution and as neat film is studied. The samples are transversally pumped with picosecond excitation pulses wavelength, 347.15 nm; duration, 35 ps. Lasing occurs at 401 nm for TPD in 1,4-dioxane and at 418 nm for TPD neat films. For the photo-physical characterization, the optical constants of neat films are determined by reflection and transmission measurement, the absorption cross-sections are extracted, and fluorescence spectroscopic parameters are determined. The fluorescence quantum yield of TPD in 1,4-dioxane is 0.69 and for neat TPD films, the fluorescence quantum yield is 0.31. q 2000 Elsevier Science S.A. All rights reserved.

Keywords: Travelling-wave lasing; Amplified spontaneous emission; Triphenylamine dimer TPD; TPD neat films; Optical constants; Absorption cross-sections; Fluorescence quantum yields

1. Introduction

Thin films of the aromatic diamine molecule *N,N*′-diphenyl-bis 3-methylphenyl -biphenyl-4,4′-diamine, TPD are widely used as hole-transport layers HTL in organic light emitting diodes OLEDs [1–9]. Their absorption behaviour [10,11] and emission behaviour [10] has been studied. Recently, whispering-gallery mode lasing [12,13] of a TPD coated optical fiber has been reported [14].

Here, absorption and emission spectroscopic parameters of TPD in liquid solution solvent 1,4-dioxane and of TPD neat films on fused silica substrates are determined and amplified spontaneous emission ASE studies on TPD in 1,4-dioxane and on TPD neat films are performed. The studies here show that TPD molecules have high fluorescence quantum yields in liquid solution and in neat films. Travelling-wave lasing is achieved here both for liquid solution and neat films.

Generally in organic laser dyes aggregation occurs at high concentration, and the fluorescence efficiency is strongly reduced in highly concentrated solutions and in neat films [15–17]. No lasing action has been reported in organic laser dye neat films. Only recently ASE of thin films was reported for several spiro-type dyes [18,19].

Contrary to the monomeric organic laser dyes, several luminescent polymers have high fluorescence quantum yields in solution and as neat films and allow laser action in solutions and neat films see [20–24] and references therein. For the class of triphenylamine polymers ASE has already been achieved for poly *N,N*′-diphenyl-*N,N*′-bis 3-methylphenyl -biphenyl-4,4′-diamine-co-diphenylxylylene poly-TPD-DPX [25], poly *N,N*′-diphenyl-*N,N*′-bis 4-methylphenyl -biphenyl-4,4′-diamine-co-diphenylxylylene poly 4-MeTPD-DPX [26] neat film ASE peak emission wavelength λ_{ASE} 422 nm, own unpublished results, and poly[phenylimino-4,4′-diphenylene -phenylmino-3-methyl-1,4-phenylene-1,2-ethenylene-2,5-dioctylixy-1,4-phenylene-1,2-ethenylene-2-methyl-1,4-

* Corresponding author. Tel.: q49-941-943-2107; fax: q49-941-943-2754.
E-mail address: alfons.penzkofer@physik.uni-regensburg.de (A. Penzkofer).

0379-6779/00/$ - see front matter
PII: S0379-6779(00)00231-9

phenylene-TPD-PPV [27] neat film ASE peak emission wavelength λ_{ASE} = 537 nm, own unpublished results).

2. Experimental

Thin films on fused silica were formed by dissolving the material in toluene (20 mg TPD per 1 ml toluene) and spin-coating the solution on the substrate. For liquid solution studies, TPD was dissolved in analytical grade 1,4-dioxane. The chemicals were purchased from Aldrich (solvents) and SynTec, Wolfen, Germany. They were used without further purification. The structural formula of TPD is displayed in Fig. 1.

The travelling-wave lasing studies are carried out by transversally exciting the samples with single picosecond frequency-doubled pulses of an active and passive mode-locked ruby laser [28] (pulse duration Δt_L = 35 ps, wavelength λ_L = 347.15 nm, pulse energy up to W_L = 1 mJ). The samples are transversally pumped. The pump beam profiles at the film position are elongated along the ASE-optical axis to 10.4 mm (FWHM) and narrowed transverse it to 0.245 mm with cylindrical lenses. The emitted ASE signal is collimated and directed to a spectrometer-diode-array detection system (observation of spectral amplification and spectral narrowing) and to a temporal signal detection system consisting of a fast micro-channelplate photomultiplier (Hamamatsu type R1564U-01) and a fast real time digital oscilloscope (LeCroy type 9362) (observation of signal amplification and ASE pulse duration measurement). The experimental procedure and the experimental setup are described in Refs. [23,24]. The optical constants (refractive index, $n(\lambda)$, and absorption coefficient, $\alpha(\lambda)$) of the TPD thin films are measured by reflectance and transmittance measurements. The technique has been described previously [29,30]. The fluorescence analysis is carried out with a self-assembled fluorimeter [31]. The data analysis is described in Ref. [32]. As reference standard, we use quinine sulfate dihydrate (from Aldrich) in normal aqueous H_2SO_4 (fluorescence quantum efficiency $\Phi(C) = 0.546 / (1 + 14.5C)$ at 25°C, where C is the dye concentration in mol dm^{-3} [33]). The fluorescence lifetime measurements are carried out with the same picosecond laser excitation system and the same temporal signal detection system as the ASE measurements. Only the sample transmissions are increased to avoid amplification of spontaneous emission.

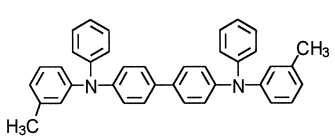

TPD

Fig. 1. Structural formula of TPD.

3. Results

3.1. Spectroscopic characterization

The reflectance and transmittance spectra of a 59 nm thick TPD film on a fused silica substrate are shown by the solid curves in Fig. 2. The dashed curves display the reflectance and transmittance of the fused silica substrate. The absorption cross-section spectrum, $\alpha(\lambda)$, and the refractive index spectrum, $n(\lambda)$, derived from Fig. 2 are displayed in Fig. 3 (procedure described in Refs. [29,30]). The absorption spectrum has a maximum at 353 nm. The refractive index dispersion peaks at 379 nm. The refractive index dispersion of fused silica is shown by the dashed curve in Fig. 3b. The refractive index spectrum of the TPD film is considerably larger than the refractive index spectrum of the fused silica substrate in the displayed wavelength region.

Waveguiding is allowed in the asymmetric planar structure of substrate-film-air beyond a critical film thickness of [34]

$$d_{crit} = \frac{\lambda}{2\pi\sqrt{n_f^2 - n_s^2}} \arctan\left(\frac{n_s^2 - 1}{n_f^2 - n_s^2}\right)^{1/2}, \qquad (1)$$

where λ is wavelength, n_f and n_s are the refractive indices of the film and the substrate, respectively. At λ = 418 nm as the wavelength of peak ASE (see below Fig. 5a), the refractive indices are n_f = 1.86 and n_s = 1.4686 giving d_{crit} = 38.5 nm.

The absorption cross-section spectra, $\sigma_a(\lambda)$ of TPD in 1,4-dioxane (dashed curve) and of TPD neat films (solid curve) are shown in Fig. 4. For the liquid solution $\sigma_a(\lambda)$ is determined from transmission measurements, i.e. $T(\lambda) = \exp(-\sigma_a(\lambda) N_0 l)$, where N_0 is the number density of TPD molecules and l is the sample length. The absorption cross-section spectrum of the neat film is determined by assuming equal absorption cross-section integrals in the wavelength region from 260 to 410 nm. The relation $\sigma_{a,f}(\lambda) = \alpha_f(\lambda) \cdot \int_{a,s}(\tilde{\nu}) d\tilde{\nu} / \int \alpha_f(\tilde{\nu}) d\tilde{\nu}$ is used, where $\tilde{\nu} = \lambda^{-1}$ is the wavenumber. The assumption of equal absorption cross-section integrals is reasonable since the absorption integrals or oscillator strengths of the allowed transitions depend little on solvent and concentration [35,36].

The fluorescence quantum yield measurements [32] give $\Phi_F = \int_{em} E_F(\lambda) d\lambda$ = 0.69 for 3.6×10^{-5} molar TPD in 1,4-dioxane and Φ_F = 0.40 for a 50 nm thick neat film. The normalized fluorescence quantum distributions, $E_F^x(\lambda) = E_F(\lambda) / E_F(\lambda_{max,F})$, are displayed in Fig. 5a. The fluorescence quantum distribution of the neat film (solid curve) is slightly red shifted compared to fluorescence quantum distribution of the liquid solution (dashed curve) as is the absorption cross-section spectrum (Fig. 4).

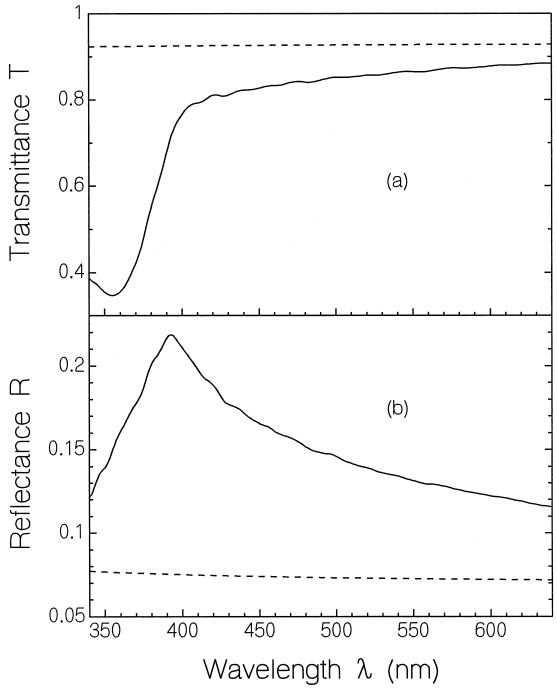

Fig. 2. a. Transmittance, $T(\lambda)$, and b. reflectance, $R(\lambda)$, of a 59 nm thick spin-coated neat thin film of TPD on fused silica (solid curves). The dashed curves show the transmittance and reflectance values of the fused silica substrate.

Temporal fluorescence signals of a 5×10^{-7} molar TPD solution in 1,4-dioxane and of a TPD neat film are displayed in Fig. 6a and b, respectively (dash-dotted curves). The dotted curves in Fig. 6a and b show the temporal response of the detection system which was determined by directing a small amount of the pump laser light to the detector. The deconvoluted fluorescence lifetimes are $\tau_{F,s} = 1.24 \pm 0.05$ ns and $\tau_{F,f} = 440 \pm 100$ ps for the solution and the film, respectively.

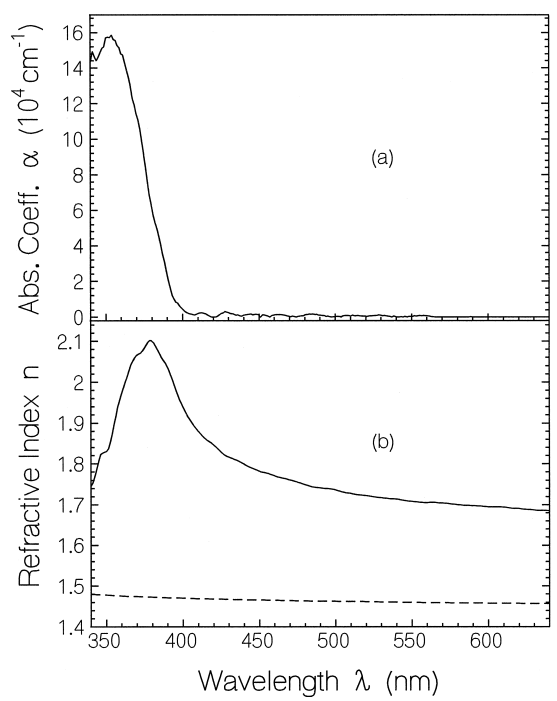

Fig. 3. a. Absorption coefficient spectrum, $\alpha(\lambda)$, and b. refractive index spectrum, $n(\lambda)$, of TPD neat thin films (solid curves). The dashed curve in b. is the refractive index spectrum of the fused silica substrate.

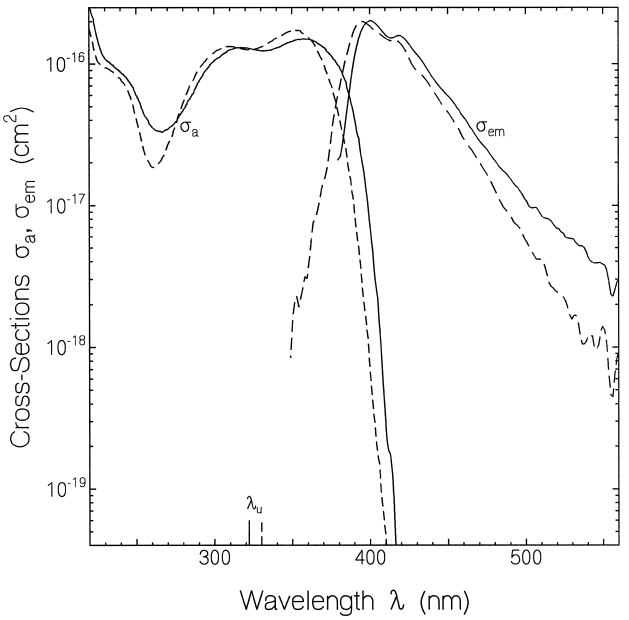

Fig. 4. Absorption cross-section spectra, $\sigma_a(\lambda)$, and stimulated emission cross-section spectra, $\sigma_{em}(\lambda)$, of TPD neat thin films (solid curves) and of TPD in 1,4-dioxane (dashed curves, concentration $C = 3.6 \times 10^{-5}$ mol dm^{-3}).

The radiative lifetime, τ_{rad} of TPD is obtained by the ratio $\tau_{rad} = \tau_F / \Phi_F$, giving $\tau_{rad,s} = 1.8$ ns and $\tau_{rad,f} = 1.1$ ns. The radiative lifetime is related to the S_0–S_1-absorption cross-section spectrum by the Strickler–Berg formula [37,38]

$$\tau_{rad} = \left[\frac{8\pi c_0 n_F^3}{n_A} \frac{\int_{em} E_F^*(\lambda)\,d\lambda}{\int_{em} E_F^*(\lambda)\,\lambda^3\,d\lambda} \int_{abs} \frac{\sigma_a(\lambda)}{\lambda}\,d\lambda \right]^{-1}, \quad (2)$$

where the integrals extend over the regions of $S_1 \rightarrow S_0$ emission (em) and $S_0 \rightarrow S_1$ absorption (abs). n_F and n_A are the average refractive indices in the S_0–S_1 fluorescence and absorption region. c_0 is the vacuum light velocity. Eq. (2) gives the experimental radiative lifetimes $\tau_{rad,f}$ and $\tau_{rad,s}$ if the upper wavelength integration border, λ_u, of the S_0–S_1 absorption is set to $\lambda_u = 322$ nm and $\lambda_u = 330$ nm for the neat film and the solution, respectively.

The stimulated emission cross-section spectra, $\sigma_{em}(\lambda)$, are derived from the radiative lifetime and the fluorescence quantum distribution by use of the Einstein relation [39,40]

$$\sigma_{em}(\lambda) = \frac{\lambda^4}{8\pi n_F^2 c_0 \tau_{rad}} \frac{E_F^*(\lambda)}{\int_{em} E_F^*(\lambda)\,d\lambda}. \quad (3)$$

The result is shown in Fig. 4. The absorption cross-section spectrum and the stimulated emission cross-section spectrum of the neat films are slightly red shifted compared to the 1,4-dioxane solutions.

In Fig. 5b, distributions of the degree of fluorescence polarization [41]

$$P_F(\lambda) = [S_{F,\parallel}(\lambda) - S_{F,\perp}(\lambda)]/[S_{F,\parallel}(\lambda) + S_{F,\perp}(\lambda)], \quad (4)$$

are shown. $S_{F,\parallel}(\lambda)$ is the fluorescence spectrum polarized parallel to the excitation light polarization, and $S_{F,\perp}(\lambda)$ is the fluorescence spectrum polarized perpendicular to the excitation light polarization. The degree of fluorescence polarization, P_F, is related to the reorientation time, τ_{or}, of the transition dipole moments by [41,42]

$$\tau_{or} = \frac{1/P_{F,0} - 1/3}{1 - P_F/P_{F,0}} P_F \tau_F, \quad (5)$$

where $P_{F,0} = 0.5$ is the limiting degree of fluorescence polarization without transition dipole reorientation ($\tau_{or} = \infty$). From Fig. 5b, we find $P_{F,s} = 0.14$, $P_{F,f} = 0.01$ and obtain $\tau_{or,s} = 400$ ps, $\tau_{or,f} = 8$ ps for 3.6×10^{-5} molar TPD in 1,4-dioxane and for a TPD neat film, respectively. In the liquid solution, the value of τ_{or} is due to molecular reorientation, while in the neat film the small value of τ_{or} is due to excitation transfer between neighboring TPD molecules.

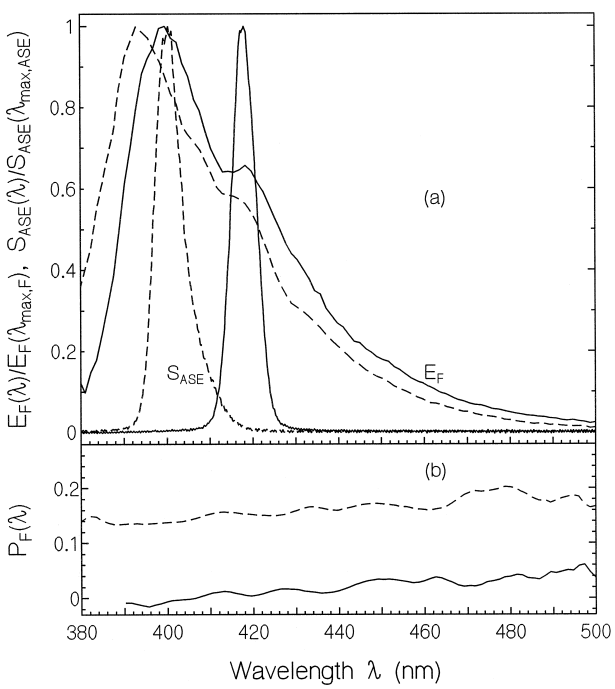

Fig. 5. a. Normalized fluorescence quantum yield distributions, $E_F(\lambda)/E_F(\lambda_{max,F})$, and normalized ASE spectra, $S_{ASE}(\lambda)/S_{ASE}(\lambda_{max,ASE})$ of TPD neat thin films (solid curves) and of TPD in 1,4-dioxane (dashed curves) at room temperature. The sample parameters for the ASE measurements are for the solution: $C = 2.4 \times 10^{-3}$ mol dm^{-3}, $d = 1$ mm, $l = 5$ mm; and for the neat film: $d = 66$ nm, $l = 10$ mm. The pump pulse energy density was $w_L = 3$ mJ cm^{-2}. b. Spectral distributions of the degree of fluorescence polarization of 3.6×10^{-5} molar TPD in 1,4-dioxane (dashed curve) and of a 55 nm thick TPD neat film (solid curve).

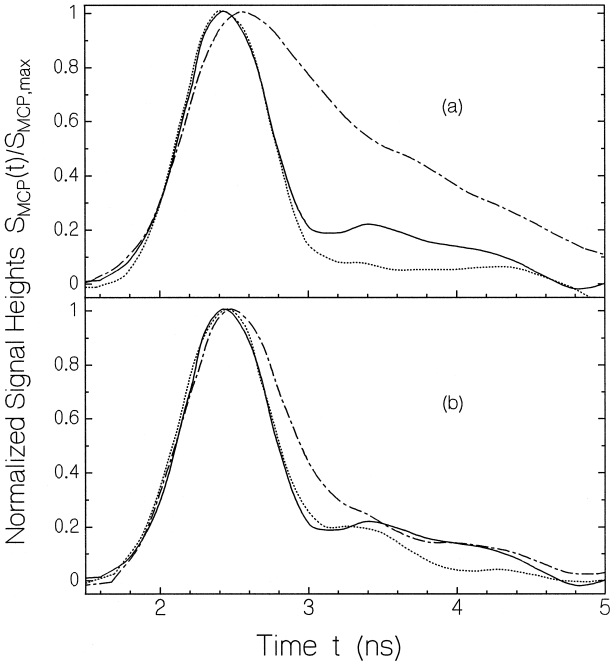

Fig. 6. Temporal fluorescence and ASE signal traces. a. TPD in 1,4-dioxane. Solid curve, instrumental response function. Dash-dotted curves, fluorescence signal of 3.6×10^{-5} molar solution. Dotted curve, ASE signal belonging to 2.4×10^{-3} molar solution in cell of 5 mm length, pump pulse energy of 800 mJ, and pump pulse area of 10.4×0.245 mm^2. b. TPD neat thin film. Solid curve, instrumental response function. Dash-dotted curve, fluorescence signal of 4 nm thick film. Dotted curve, ASE signal of 66 nm thick film (pump pulse energy, 230 mJ; pump pulse area, 10.4×0.245 mm^2).

3.2. Trapping-waveguiding

In Fig. 5a, ASE spectra for a 2.4×10^{-3} molar solution of TPD in 1,4-dioxane (sample length $l = 5$ mm, cell thickness $d = 1$ mm, excitation energy $W_L = 800$ mJ, sharp dashed curve) and for a neat thin TPD film (sample length $l = 10$ mm, film thickness $d = 66$ nm, $W_L = 230$ mJ, sharp solid curve) are shown. The pump laser cross-section at the sample position was 10.4 mm × 0.245 mm (FWHM). The spectral peak positions and the spectral half-widths of the ASE spectra are $\lambda_{max,ASE,s} = 401$ nm, $\Delta\lambda_{ASE,s} = 7.2$ nm, $\lambda_{max,ASE,f} = 418$ nm, and $\Delta\lambda_{ASE,f} = 6.6$ nm for the solution (s) and the film (f), respectively. In the solution, the ASE spectrum is slightly red shifted compared to the fluorescence peak. For the neat film, the ASE spectrum is positioned at the vibronic peak of the fluorescence spectrum. The long-wavelength shift of the ASE spectra compared to the stimulated emission cross-section peaks (Fig. 4) is

caused by the residual ground-state absorption Fig. 4. which decreases with rising wavelengths. The spectral shapes and widths of the ASE spectra are determined by the gain narrowing effect of amplification based on the effective stimulated emission cross-section distribution and the level population dynamics [43–46].

The excitation light was vertically polarized. The long-axis of the line-shaped excitation laser beam profile at the samples was in the horizontal direction. The ASE propagated along the long-axis of the pump beam and remained the vertical polarization of the excitation beam.

The temporal ASE-signals for the solution and the neat film are included in Fig. 6a and b, respectively solid curves. The ASE pulse shapes approximately coincide with the system response function. The ASE pulse durations, Δt_{ASE}, may be comparable to the pump pulse duration, Δt_L [44].

The spectral signal eight, $S(\lambda_{max,ASE})$, versus input pump pulse energy density, w_L, is shown in Fig. 7a for the solution and in Fig. 7b for the neat film. Only the low pump energy density range is displayed. At the beginning, the signal is dominated by spontaneous emission. Then the steep rise in the signal indicates the dominance of ASE. For the 2.4×10^{-3} molar TPD solution, the ASE onset pump pulse energy density is approximately 0.3 mJ/cm^2, while for the neat film the onset pump pulse energy density is approximately 20 mJ/cm^2.

In Fig. 7c and d, the spectral halfwidth, $\Delta\lambda$, FWHM. of the emission versus input pump pulse energy density is displayed. In a small pump pulse energy region, $\Delta\lambda$ narrows from the fluorescence linewidth to the ASE linewidth. The energy density positions, $w_{L,1/2}$, where the linewidth is narrowed to half its initial linewidth are indicated to be 0.33 mJ/cm^2 for the solution and 20 mJ/cm^2 for the neat film.

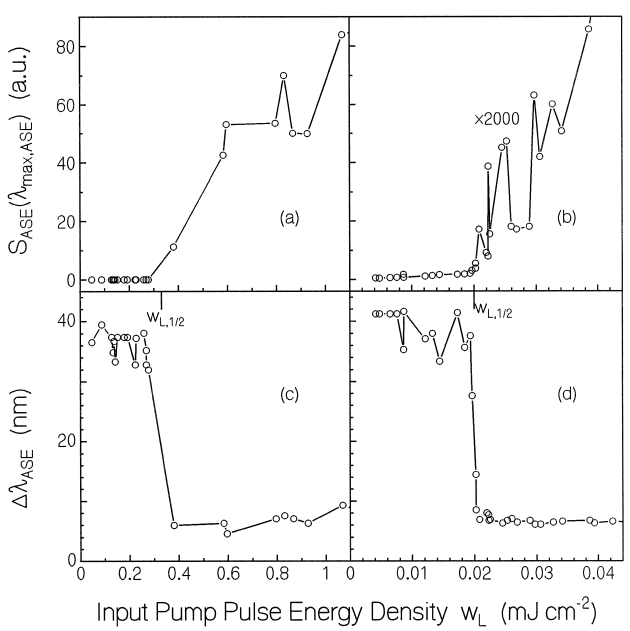

Fig. 7. Amplified spontaneous emission characteristics of TPD neat films b,d. film thickness 66 nm. and 1,4-dioxane solutions a,c. concentration 2.4×10^{-3} mol dm^{-3}. a,b. Maximum spectral height of emission versus peak input pulse energy density. c,d. Spectral width of emission FWHM. versus peak input pump pulse energy density.

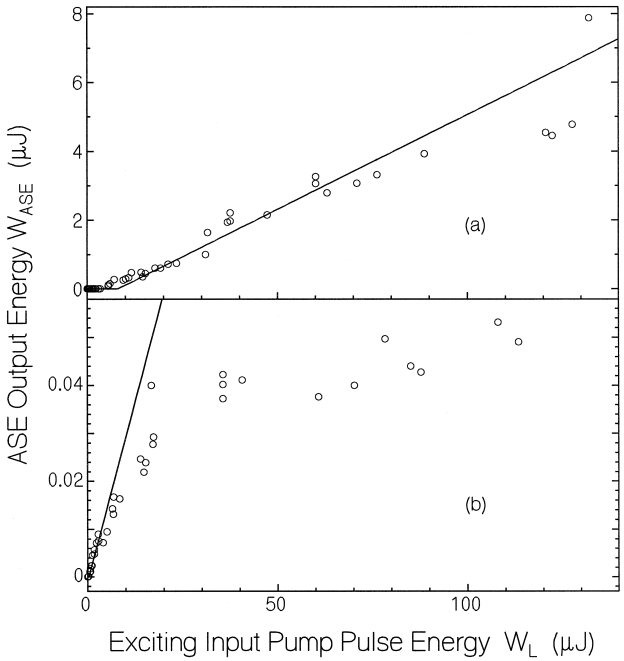

Fig. 8. Travelling-wave laser output energy, W_{ASE}, in one direction versus input energy, W_L, hitting the samples. a. 2.4×10^{-3} molar TPD in 1,4-dioxane. Sample length, l 5 mm. Cell thickness, d 1 mm. Solid line, $W_{ASE} = 0.055\ W_L - 8$ mJ. b. 66 nm thick neat film of TPD on fused silica. Sample length l 10 mm. Solid line, $W_{ASE} = 0.003\ W_L - 0.3$ mJ.

The ASE output energy, W_{ASE}, emitted along one direction of the excitation path versus the input pump pulse energy, W_L, hitting the sample is plotted in Fig. 8a for the solution and in Fig. 8b for the neat film. The solid angle of light collection was 2.8×10^{-2} sr. For the solution Fig. 8a., the one-directional laser slope efficiency is $\eta_{sl} = 0.055$ $\eta_{sl} = 0.11$ considering both emission directions. A threshold for the onset of ASE is observed, and then the output ASE energy rises linearly with the input pump pulse energy linearity was tested up to $W_L = 450$ mJ. For the neat film the threshold of ASE is 0.3 mW. It is not resolved on the abscissa scale of Fig. 8. The ASE signal begins to saturate for $W_L > 5$ mJ probably due to heating of the pumped thin film volume. At low pump pulse energy the laser slope efficiency is $\eta_{sl} = 0.003$.

4. Discussion

The amplification of spontaneous emission of TPD in neat films and in solution is discussed.

Table 1
Spectroscopic and amplified spontaneous emission parameters of TPD

Parameter	Neat film	1,4-Dioxane solution	Comment
f_F	0.40	0.69	
t_{rad} ns	1.1	1.8	$t_{rad} = t_F / f_F$
t_F ns	0.44	1.4	
t_{or} ps	8	400	Eq. (5)
$\sigma_{L,a}$ cm^2	1.41×10^{-16}	1.68×10^{-16}	Fig. 4
w_{sat} J cm^{-2}	4.1×10^{-3}	3.4×10^{-3}	$w_{sat} = h\nu_L / \sigma_{L,a}$ (7)
$w_{L,1/2}$ J cm^{-2}	2×10^{-5}	3.3×10^{-4}	Fig. 7
η_{sl}	0.003	0.055	Fig. 8
$\lambda_{max,ASE}$ nm	418	401	Fig. 5a
$\sigma_a(\lambda_{max,ASE})$ cm^2	10^{-20}	5.1×10^{-19}	Fig. 4
$\sigma_{em}(\lambda_{max,ASE})$ cm^2	1.6×10^{-16}	1.83×10^{-16}	Fig. 4
N_0 cm^{-3}	1.06×10^{21}	1.45×10^{18}	
l mm	10	5	
l_{ASE} mm	0.9	5	
$d_{abs,L}$ mm	0.067	41	$(\sigma_a(\lambda_L) \cdot N_0)^{-1}$
d mm	0.066	1000	
d_{eff} mm	0.22	41	
$\sigma_{em,eff}(\lambda_{max,ASE})$ cm^2	4.9×10^{-17}	9.8×10^{-17}	Eq. (6)
f_{em}	0.3	0.54	$\sigma_{em,eff}(\lambda_{max,ASE}) / \sigma_{em}(\lambda_{max,ASE})$

At the pump pulse energy density, $w_{L,1/2}$, of 50% spectral narrowing onset of efficient ASE, a pump pulse induced ground-state depopulation is negligible, because the saturation energy density [47], $w_{sat} = h\nu_L / \sigma_{L,a}$, of ground-state depopulation is large compared to $w_{L,1/2}$ ($\nu_L = C_0 \lambda_L^{-1}$ is laser frequency, $\sigma_{L,a}$ is absorption cross-section at ν_L). Data of w_{sat} and $w_{L,1/2}$ are given in Table 1.

Neglecting ground-state depletion, the ground-state absorption length at the wavelength of peak ASE is $l_{abs} = (\sigma_a(\lambda_{max,ASE}) \cdot N_0)^{-1}$, where N_0 is the TPD molecule number density. The effective gain length, l_{ASE}, is given by the minimum of the sample length, l, and the absorption length, l_{abs}. The experimental parameters of $\sigma_a(\lambda_{max,ASE})$, N_0, l, and l_{ASE} are listed in Table 1. For the applied solution l_{ASE} is given by the sample length $l = 5$ mm, while for the neat film, l_{ASE} is given by the absorption length, $l_{abs} = 0.9$ mm.

The lasing efficiency depends on the stimulated emission cross-section, σ_{em}, and the excited-state absorption cross-section, σ_{ex}, at the laser wavelength region. The effective stimulated emission cross-section, $\sigma_{em,eff}(\lambda_{max,ASE}) = \sigma_{em}(\lambda_{max,ASE}) - \sigma_{ex}(\lambda_{max,ASE})$, may be determined from the pump pulse energy density, $w_{L,1/2}$, necessary for spectral narrowing the emission by a factor of two. A relation for $\sigma_{em,eff}(\lambda_{max,ASE})$ has been derived in Ref. [24], which reads for a pump laser penetration depth, $d_{abs,L} = (N_0 \sigma_a(\lambda_L))^{-1}$, smaller than the sample thickness, d, and negligible ground-state depletion at $w_L = w_{L,1/2}$

$$\sigma_{em,eff}(\lambda_{max,ASE}) = \frac{\ln 2 \cdot h\nu_L d_{eff}}{(1 - \exp(-0.25 \ln 2 \cdot 4 w_{L,1/2} / l_{ASE}))(1 - \exp(-N_0 \sigma_a(\lambda_L) d))}, \quad (6)$$

where d_{eff} is the width of the ASE light in the sample pump laser penetration depth, $d_{abs,L}$, in the case of liquid solutions with $l_L < d_{abs,L} - d$, or effective width of guided light in thin film due to Goos–Haenchen effect [48]. d is the minimum of either d_{eff} or d. Experimental d and d_{eff} values and calculated $\sigma_{em,eff}(\lambda_{max,ASE})$ values are listed in Table 1. The ratio, $f_{em} = \sigma_{em,eff}(\lambda_{max,ASE}) / \sigma_{em}(\lambda_{max,ASE})$, which may be considered as a stimulated-emission figure of merit is found to be $f_{em,s} = 0.54$ for the 1,4-dioxane solution and $f_{em,f} = 0.30$ for the neat film.

In Ref. [25], the travelling-wave lasing behaviour of poly-TPD-DPX, a copolymer of TPD and α,α-diphenylxylylene, has been studied in detail. The laser performance data of the TPD molecule solutions and neat films are slightly better than the corresponding data for poly-TPD-DPX solutions and neat films ($\eta_{sl,s} = 0.05$, $\eta_{sl,f} = 7 \times 10^{-5}$, $f_{em,s} = 0.14$, $f_{em,f} = 0.055$). But poly-TPD-DPX forms very smooth films on glass substrates and has a high glass transition temperature of $T_g = 240$°C which is important for electrical pumping of thin films towards light emission and amplification of light emission.

5. Conclusions

The optical constants, the fluorescence properties, and the travelling-wave lasing behaviour of the aromatic diamine molecule TPD have been studied. The travelling-wave lasing of TPD in liquid solution is similar to the travelling-wave lasing of organic laser dyes in liquid solution under similar pumping conditions [44,49]. But wave-guided travelling-wave lasing in neat thin films obtained here for TPD has not reported to occur in neat thin films of

organic laser dyes. In TPD neat films, the fluorescence yield is high $f_{F,f}$ 0.3, while in neat films of organic laser dyes, it is generally very low for example $f_{F,f}$ 0.004 for rhodamine 6G neat films [17].

Acknowledgements

The authors thank the Commission of the European Communities for support under ESPRIT contract 28580 ''A Novel Approach to Solid State Short Wavelength Laser Generation Using Luminescent Polymers LUPO.'' which enabled this collaborative work.

References

[1] C.W. Tang, S.A. Van Slyke, Appl. Phys. Lett. 51 1987 913.
[2] C.W. Tang, S.A. Van Slyke, C.H. Chen, J. Appl. Phys. 65 1989 3610.
[3] C. Adachi, T. Tsutsui, S. Saito, Appl. Phys. Lett. 55 1989 1489.
[4] C. Adachi, T. Tsutsui, S. Saito, Appl. Phys. Lett. 56 1990 799.
[5] Y. Ohmori, A. Fujii, M. Uchida, C. Morishima, K. Yoshino, Appl. Phys. Lett. 62 1993 3250.
[6] Y. Ohmori, A. Fujii, M. Uchida, C. Morishima, K. Yoshino, J. Phys. Condens. Mater. 5 1993 7979.
[7] J. Kido, H. Hayase, K. Hongawa, K. Nagai, Okuyama, Appl. Phys. Lett. 65 1994 2124.
[8] R.H. Jordan, L.J. Rothberg, A. Dodabalapur, R.E. Slusher, Appl. Phys. Lett. 69 1996 1997.
[9] S. Okutso, T. Onikubo, M. Tamano, T. Enokida, IEEE Trans. Electron Devices 44 1997 1302.
[10] S. Pfeiffer, H.-H. Hörhold, H. Boerner, H. Nikol, W. Busselt, SPIE 3476 1998 258.
[11] N. Tada, S. Tatsuhara, A. Fujii, Y. Ohmori, K. Yoshino, Jpn. J. Appl. Phys. 36 1997 L421.
[12] S.V. Frolov, M. Shkunov, Z.V. Vardeny, K. Yoshiniv, Phys. Rev. B 56 1997 R4363.
[13] Y. Kawabe, Ch. Spielgelberg, A. Schülzgen, M.F. Nabor, B. Kippelen, E.A. Mash, P.M. Allemand, M. Kuwata-Gonokami, K. Takeda, N. Peygahmbarian, Appl. Phys. Lett. 72 1998 141.
[14] Y. Kawabe, C. Spiegelberg, A. Schuelzgen, M.F. Nabor, G.F. Nabor, G.E. Jabbor, B. Kippelen, E.A. Mash, P.M. Allemand, N. Peyghambarian, M. Kuwata-Gonokami, K. Takeda, Proc. SPIE 3281 1998 211.
[15] Dye Lasers, 2nd revised edn., F.P. Schäfer Ed., Topics in Applied Physics vol. 1 Springer-Verlag, Berlin, 1977.
[16] F.J. Duarte, L.W. Hillman Eds., Dye Laser Principles with Applications, Academic Press, Boston, 1990.
[17] A. Penzkofer, Y. Lu, Chem. Phys. 103 1986 399.
[18] N. Johansson, J. Salbeck, J. Bauer, F. Weissörtel, P. Broms, A. Anderson, W.R. Salaneck, Synth. Met. 101 1999 405.
[19] N. Johansson, J. Salbeck, J. Bauer, F. Weissörtel, P. Broms, A. Anderson, W.R. Salaneck, Adv. Mater. 10 1998 1136.
[20] N. Tessler, G.I. Denton, R.H. Friend, Nature 382 1996 695.
[21] M.D. McGehee, M.A. Díaz-García, F. Hide, R. Gupta, E.K. Müller, D. Moses, A.J. Heeger, Appl. Phys. Lett. 72 1998 1536.
[22] C. Kallinger, M. Hilmer, A. Haugeneder, M. Perner, W. Spirkl, U. Lemmer, J. Feldmann, U. Scherf, K. Müllen, A. Gombert, V. Wittwer, Adv. Mater. 10 1998 920.
[23] A. Penzkofer, W. Holzer, S.-H. Gong, D.D.C. Bradley, X. Long, A. Bleyer, W.J. Blau, A.P. Davey, in: V.J. Corcoran, T.A. Goldman Eds., Proc. Int. Conf. Lasers '98, STS Press, McLean, VA, 1999, p. 394.
[24] W. Holzer, A. Penzkofer, T. Schmitt, A. Hartmann, C. Bader, H. Tillmann, D. Raabe, R. Stockmann, H.-H. Hörhold, Amplified spontaneous emission in neat films of arylene-vinylene polymers, Opt. Quantum Electron., submitted for publication.
[25] W. Holzer, A. Penzkofer, H.-H. Hörhold, D. Raabe, M. Helbig, Photophysical and lasing characterization of an aromatic diamine-xylylene copolymer, Opt. Mater., in press.
[26] H.H. Hörhold et al., Synthesis of poly 4-MeTPD-DPX, unpublished.
[27] H. Rost, H.H. Hörhold, W. Kreuder, H. Spreitzer, Proc. SPIE 3148 1997 373.
[28] P. Weidner, A. Penzkofer, Opt. Quantum Electron. 25 1993 1.
[29] A. Penzkofer, E. Drotleff, W. Holzer, Opt. Commun. 158 1998 221.
[30] W. Holzer, M. Pichlmaier, E. Drotleff, A. Penzkofer, D.D.C. Bradley, W.J. Blau, Opt. Commun. 163 1999 24.
[31] A. Penzkofer, W. Leupacher, J. Lumin. 37 1987 61.
[32] W. Holzer, M. Pichlmaier, A. Penzkofer, D.D.C. Bradley, W.J. Blau, Chem. Phys. 246 1999 445.
[33] W.H. Melhuish, J. Phys. Chem. 72 1968 2680.
[34] H. Kogelnik, in: T. Tamir Ed., Integrated Optics, Topics in Applied Physics vol. 7 Springer-Verlag, Berlin, 1979, p. 13.
[35] J.B. Birks, in: Photophysics of Aromatic Molecules, Wiley, London, 1970, p. 51.
[36] N.J. Turro, in: Modern Molecular Photochemistry, Benjamin Cummigns Publishing, Menlo Park, CA, 1978, p. 86.
[37] S.J. Strickler, R.A. Berg, J. Chem. Phys. 37 1962 814.
[38] J.B. Birks, D.J. Dyson, Proc. R. Soc. London, Ser. A 275 1963 135.
[39] O.G. Peterson, J.P. Webb, W.C. McColgin, J.H. Eberly, J. Appl. Phys. 42 1971 1917.
[40] A.V. Deshpande, A. Beidoun, A. Penzkofer, G. Wagenblast, Chem. Phys. 142 1990 123.
[41] J.R. Lakowicz, Principles of Fluorescence Spectroscopy, Plenum, New York, 1983.
[42] F. Ammer, A. Penzkofer, P. Weidner, Chem. Phys. 192 1995 325.
[43] A. Penzkofer, W. Falkenstein, Opt. Quantum Electron. 10 1978 399.
[44] W. Falkenstein, A. Penzkofer, W. Kaiser, Opt. Commun. 27 1978 151.
[45] G. Wegmann, B. Schweitzer, D. Hertel, H. Gressen, M. Oestreich, U. Scherf, K. Müllen, R.F. Mahrt, Chem. Phys. Lett. 312 1999 376.
[46] T.-A. Pham, T. Barisien, V. Grayer, L. Guidoni, G. Hadziioannou, J.-Y. Bigot, Chem. Phys. Lett. 318 2000 459.
[47] H. Hercher, Appl. Opt. 6 1967 947.
[48] M.J. Adams, in: An Introduction to Optical Waveguides, Wiley, Chichester, 1981, p. 23.
[49] J. Klebniczki, Zs. Bor, G. Szabo, Appl. Phys. B 46 1988 151.